Pharm Res (2012) 29:3512–3525
DOI 10.1007/s11095-012-0848-8

RESEARCH PAPER

Biodegradable Polymer-Curcumin Conjugate Micelles Enhance the Loading and Delivery of Low-Potency Curcumin

Rulei Yang • Suai Zhang • Deling Kong • Xuli Gao • Yanjun Zhao • Zheng Wang

Received: 15 March 2012 / Accepted: 31 July 2012 / Published online: 15 August 2012

ABSTRACT

Purpose To utilize a novel type of polymer-drug conjugate micelle to enhance the delivery of low-potency curcumin.

Methods Multiple curcumin molecules were conjugated to poly (lactic acid) (PLA) via tris(hydroxymethyl)aminomethane (Tris) linker producing the hydrophobic drug-binding block; methoxy-poly(ethylene glycol) (mPEG) was employed as the hydrophilic block. Micelles were characterized by size, loading capacity, stability, and critical micelle concentration (CMC). Human hepatocellular carcinoma (HepG2) cells were employed to assess cytotoxicity and intracellular targeting ability of micelles.

Results mPEG-PLA-Tris-Cur micelles were within nanorange (<100 nm). CMC of such micelles (2.3 ± 0.4 μg/mL) was 10 times lower than mPEG-PLA micelles (27.4 ± 0.8 μg/mL). Curcumin loading in mPEG-PLA-Tris-Cur micelles reached 18.5 ± 1.3% (w/w), compared to traditional mPEG-PLA micelles at 3.6 ± 0.4% (w/w). IC_{50} of mPEG-PLA-Tris-Cur micelles (~22 μg/mL at curcumin-equivalent dose) was similar to unmodified curcumin. Placebo and drug-encapsulated conjugate micelles could be efficiently internalized to cytoplasmic compartment of HepG2 cells.

Conclusions Micelle-forming polymer-drug conjugates containing multiple drug molecules were an efficient means to increase loading and intracellular delivery of low-potency curcumin.

KEY WORDS curcumin · drug loading · micelle · mPEG-PLA · polymer-drug conjugate

ABBREVIATIONS

CLSM	confocal laser scanning microscope
CMC	critical micelle concentration
Cur	curcumin
Cur-GA	mono-carboxyl-terminated curcumin
DCC	dicyclohexylcarbodiimide
DMAP	4-dimethylamino pyridine
DMEM	Dulbecco's modification of eagle's medium
DMF	N,N-dimethylformamide
EPR	enhanced permeability and retention effect
GA	gluraric anhydride
GRAS	generally regarded as safe
HepG2	human hepatocellular carcinoma cells
HPLC	high performance liquid chromatography
mPEG	methoxy-poly(ethylene glycol)
MPS	mononuclear phagocyte system
MWCO	molecular weight cut-off
NHS	N-hydroxy succinimide
NMR	nuclear magnetic resonance
PCL	polycaprolactone

Electronic supplementary material The online version of this article (doi:10.1007/s11095-012-0848-8) contains supplementary material, which is available to authorized users.

R. Yang · X. Gao · Y. Zhao (✉) · Z. Wang (✉)
Tianjin Key Laboratory for Modern Drug Delivery & High Efficiency
School of Pharmaceutical Science & Technology, Tianjin University
92 Weijin Rd., Nankai District, Tianjin 300072, China
e-mail: zhaoyj@tju.edu.cn
e-mail: wangzheng2006@tju.edu.cn

S. Zhang · D. Kong
Institute of Biomedical Engineering
Chinese Academy of Medical Sciences
Peking Union Medical College
Tianjin 300192, China

D. Kong
Key Laboratory of Bioactive Materials, Ministry of Education, College of Life Science, Nankai University
Tianjin 300071, China

PLA	poly(lactic acid)
RBC	red blood cells
THF	tetrahydrofuran
Tris	tris(hydroxymethyl)aminomethane

INTRODUCTION

An ideal anti-cancer therapy should imbed the favourable solubility, stability, toxicity, membrane permeability, and tumor-specific targeting ability to the active agent. However, such drugs seldom exist and most anti-cancer agents suffer from low aqueous solubility, rapid blood clearance, poor tumor selectivity, and considerable side-effects for normal tissues, thus leading to compromised efficacy and patient acceptance (1). Nanoparticulate systems have been increasingly popular in delivering chemotherapeutics due to their capability to enhance drug solubility and stability, prolong blood circulation, limit nonspecific uptake, improve the accumulation in tumor via enhanced permeability and retention effect (EPR) and/or active targeting, and achieve combination therapy (2–4). Many anti-cancer drugs display limited loading in nanoparticles and the drug content is generally lower than 10% (1). Therefore it has been regularly problematic to formulate and deliver low-potency chemotherapeutic agents such as curcumin, which necessitates high drug contents in the nanocarriers for a desired therapeutic outcome (5,6).

Curcumin as a natural polyphenol derived from the *Curcuma longa* exhibits a wide spectrum of pharmacological activities due to its diverse range of molecular targets. It has been embodied by FDA GRAS (generally regarded as safe) list and has been employed for the treatment of cancer and many other diseases. As a low-potency active agent, high dose of curcumin up to a daily oral administration of 12 g in human clinical study was reported to be tolerable (7). In spite of its promising anti-cancer application, the therapeutic efficacy of curcumin is limited by its very poor aqueous solubility leading to poor absorption. Moreover, upon administration rapid metabolism and elimination of curcumin contribute to its poor bioavailability (8). Various approaches have been attempted to address the above problems of curcumin including the employment of cyclodextrin (9), nanoparticles (10), and microparticles (11), the formation of polymeric prodrug or other types of conjugates (5,12–15), the use of amphiphilic copolymer micelles (16–20) to circumvent the pitfall of poor aqueous solubility, provide longer circulation and resistance to metabolic process.

Polymer-drug conjugate micelles that combine the features of polymeric micelles and prodrug together present another potential strategy for loading curcumin. Amphiphilic copolymer micelles are attractive drug delivery systems that comprise hydrophilic corona and nonpolar core. The core was used for drug encapsulation and protection; the corona minimizes the interaction between the carrier and the biocomponents (e.g. cells and proteins) to avoid the uptake of mononuclear phagocyte system (MPS) (21) and attain an ideal pharmacokinetic profile of the drug. The spontaneous self-assembly of micelles is a free energy-driven process. Taking the advantage of the hydrophobicity of the active anti-cancer agent, the drug can be conjugated to a hydrophobic polymer forming the hydrophobic block of micelles; the hydrophilic segment surrounds the core as a hydrated exterior shell (22). Such bottom-up particle engineering technique can be tailed by the choice and length of both hydrophobic and hydrophilic blocks as well as the mode of drug conjugation to the polymer backbone; therefore micelles with nanoscopic architecture and appropriate size, stability and compatibility can be generated (23,24). A previous investigation conjugated hydrophobic haloperidol to methoxy-poly(ethylene glycol)-polycaprolactone (mPEG-PCL) copolymer that formed micelles within nanorange and the drug loading in such system was about 7 times higher compared to that of traditional mPEG-PCL micelles (25).

Previous studies often conjugate one curcumin molecule to the polymer for conjugate micelle generation (5,12,14,15). It is postulated that conjugating multiple curcumin molecules to the hydrophobic polymer backbone would not only generate a more hydrophobic drug-binding block facilitating the spontaneous generation of polymer-drug conjugate micelles and enhancing the micelle stability, but also increase the drug loading via both the covalently linked and physically encapsulated form. Thus the aim of this study was to employ the above method for efficient delivery of low-potency curcumin. mPEG was used for constructing the micelle corona and multiple curcumin molecules was conjugated to biodegradable poly(lactic acid) (PLA) via the tris (hydroxymethyl)aminomethane (Tris) linker forming the hydrophobic core of micelles (Fig. 1).

MATERIALS AND METHODS

Materials

Tris(hydroxymethyl)aminomethane (Tris), 4-dimethylamino pyridine (DMAP), stannous octanoate [$Sn(Oct)_2$], N-hydroxy succinimide (NHS), dicyclohexylcarbodiimide (DCC), triethylamine (Et_3N), and glutaric anhydride (GA) (95%) were purchased from Aladdin (Shanghai, China). Curcumin (Cur) was purchased from Institute of Guangfu

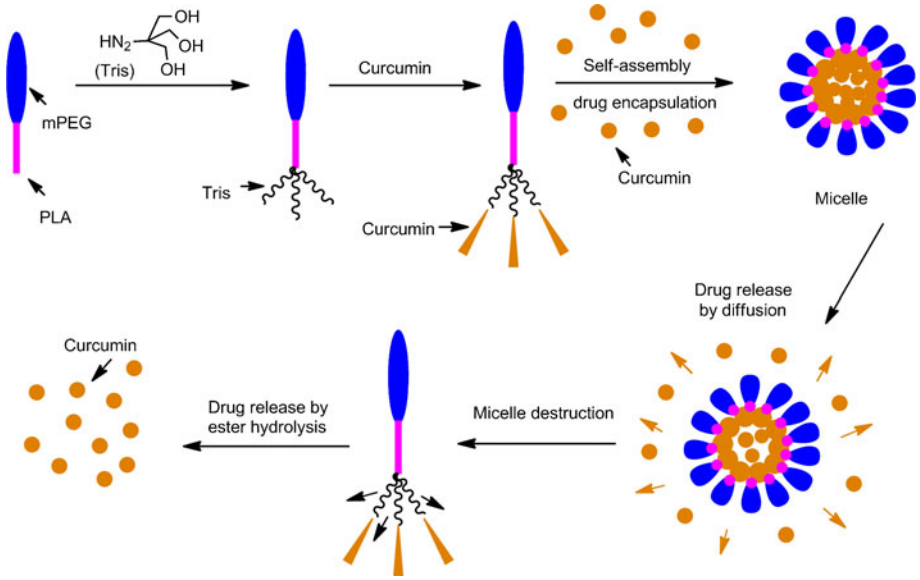

Fig. 1 Schematic illustrations of the polymer-curcumin conjugate micelles. Hydrophilic poly(ethylene glycol) (PEG) forms the corona of micelles; poly(lactic acid) (PLA) was linked with curcumin by tris (hydroxymethyl)aminomethane (Tris) generating the hydrophobic block of micelles. The self-assembly of conjugates forms micelles that contain the drug in both conjugated and encapsulated form. Drug release was achieved by diffusion and hydrolysis of ester bond. The ideal structure of mPEG-PLA-Tris-Cur was presented here and practically due to steric effect only two curcumin molecules could be conjugated to the polymer backbone.

Fine Chemical Research (Tianjin, China) and further purified by recrystallization three times in methanol and petroleum ether. Methoxy poly(ethylene glycol) with a molecular weight of 1,720 Da (M_n by gel permeation chromatography) was obtained from Sigma-Aldrich (Beijing, China), and dried by an azeotropic distillation in toluene. Anhydrous L-lactide was purchased from Yuan Shengrong (Beijing, China) and used as received. Pyrene was obtained from Yangguang Yunneng (Tianjin, China). Silica gel powder (ZCX 2) and TLC silica gel plate (GF254) were sourced from Haiyang Chemicals (Qingdao, China). Dulbecco's modification of eagle's medium (DMEM), F12K medium, fetal bovine serum, and penicillin-streptomycin were from HyClone Inc. (Logan City, Utah, USA). The human hepatocellular carcinoma cell line (HepG2) was provided by Institute of Biomedical Engineering (Chinese Academy of Medical Sciences & Peking Union Medical College). All other chemicals were of analytical grade from Jiangtian Chemicals (Tianjin, China).

Synthesis of Cur-GA

Cur-GA (mono-carboxyl-terminated curcumin) was prepared following a previously published method with slight modification (26). Curcumin (1.55 g), DMAP (0.26 g), Et_3N (0.95 mL), and tetrahydrofuran (THF) (80 mL) were mixed in a 200 mL flask followed by the addition of glutaric anhydride (0.51 g) dissolved in THF. The mixture was agitated and refluxed under nitrogen at 90°C for 17 h. The solvent was evaporated under vacuum; the crude product was re-dissolved in ethyl acetate (60 mL), and then extracted with 1 mol/L HCl (20 mL) to remove Et_3N. This process was repeated at least three times, and ethyl acetate was removed under vacuum at last to get the crude product (Scheme 1). The product (Cur-GA) was purified via silica gel column chromatography, eluted with 1,2-$C_2H_4Cl_2$:Methanol (98:2, v/v) (yield 73%). ^{1}H NMR ($CDCl_3$), (ppm): 2.11–2.15 (2H, -CH_2COOH); 2.71–2.74 (2H, -CH_2CH$_2$COOH); 2.80–2.83 (2H, -CH_2COO-); 3.90–3.97 (6H, -OCH_3); 5.85 (2H, -COCH_2CO-); 6.56–6.60 (2H, -CH=C*H*CO-); 6.95–6.97 (2H, -C*H*=C(OH)-); 7.07–7.09 (2H, =C*H*CH=C(OH)-); 7.14–7.17(2H, -C*H*=C(OCH$_3$)-); 7.61–7.65 (2H, -C*H*=CHCO-) (Figure S1, Supplementary Material).

Synthesis of mPEG-PLA

The generation of mPEG-PLA was based on minor modification of a previously published method (27). mPEG (5.0 g) was melted in a 50 mL flask following the addition of anhydrous L-lactide (5.0 g) and Sn(Oct)$_2$ (1 mL) under nitrogen; the mixture reactant was maintained at 125°C for 24 h (Scheme 1). The crude product was dissolved in THF and then purified by precipitation in ice-cooled diethyl ether followed by filtration; this process was performed in triplicate and the resultant product was vacuum-dried at ambient temperature (yield 92%). ^{1}H NMR ($CDCl_3$): (ppm): 3.66 (-CH_2CH_2O-); 3.40 (CH_3O-); 1.59 (-OCHCH_3CO-); 5.19 (-OC*H*CH$_3$CO-) (Figure S2, Supplementary Material).

Synthesis of mPEG-PLA-Cur

The generation of mPEG-PLA-Cur was achieved by the conjugation between mPEG-PLA and Cur-GA (Scheme 1). Briefly, mPEG-PLA (1.1 g) and Cur-GA (175 mg) dissolved in anhydrous methylene chloride (50 mL) were mixed with DMAP (52 mg) and DCC (108 mg). The reactants were maintained at ambient temperature for 24 h and then filtered; the filtrate was precipitated in ice-cooled diethyl

Scheme 1 The synthesis route of mPEG-PLA and mPEG-PLA-Cur.

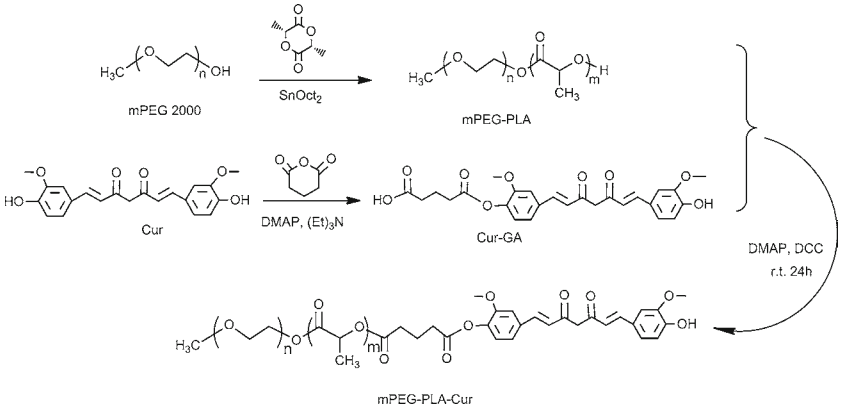

ether after condensation. The final yellow product (mPEG-PLA-Cur, yield 73%) was further purified by the dialysis method using a regenerated cellulose membrane with a molecular weight cut-off (MWCO) of 2 kD to remove the unreacted curcumin.

Synthesis of mPEG-PLA-Tris

Carboxyl-terminated mPEG-PLA (mPEG-PLA-COOH) was produced according to the literature (28). In brief, mPEG-PLA (2.0 g), succinic anhydride (68 mg), DMAP (72 mg) and Et_3N (0.15 mL) were dissolved in 1,4-dioxane (30 mL). The above solution was kept at ambient temperature for 24 h, filtered, condensed to ca. 10 mL in a rotary vacuum evaporator, and then precipitated in ice-cooled diethyl ether.

NHS was employed to activate mPEG-PLA-COOH in the presence of DCC. mPEG-PLA-COOH (1.5 g) was dissolved in methylene chloride (30 mL) and then NHS (52 mg) and DCC (112 mg) were added; the reactants were kept at 0°C with agitation. After 48 h the by-products were removed by filtration; the filtrate was condensed, precipitated in ice-cooled diethyl ether, and then vacuum-dried to get mPEG-PLA-NHS.

Tris-terminated mPEG-PLA (mPEG-PLA-Tris) was obtained through the amidation of mPEG-PLA-NHS and Tris in the presence of Et_3N in N,N-dimethylformamide (DMF). In short, mPEG-PLA-NHS (1.1 g), Tris (51 mg) and Et_3N (0.25 ml) were mixed in DMF (50 mL) at ambient temperature under stirring. After 24 h, the above solution were concentrated by rotary evaporation under vacuum, and precipitated in cold diethyl ether. This purification was carried out in triplicate followed by dialysis using a regenerated cellulose membrane (MWCO 2 kD) and freeze-drying to get mPEG-PLA-Tris (Scheme 2). The ^1H NMR spectra of mPEG-PLA-COOH and mPEG-PLA-Tris were provided in Figure S2 (Supplementary Material).

Synthesis of mPEG-PLA-Tris-Cur

Similar to the generation of mPEG-PLA-Cur, the synthesis of mPEG-PLA-Tris-Cur conjugate was achieved through the formation of ester bonds between the drug and mPEG-PLA-Tris (Scheme 2). Briefly, mPEG-PLA-Tris (0.77 g), Cur-GA (0.32 g), DMAP (0.11 g), and DCC (0.15 g) were dissolved in 50 mL anhydrous methylene chloride. The reaction was carried out at ambient temperature for 72 h. The by-products were removed by the same protocol used to purify mPEG-PLA-Cur (yield 65%).

Fluorescence Spectroscopy Analysis

Fluorescence spectra of mPEG-PLA-Cur, mPEG-PLA-Tris-Cur, and pure curcumin were recorded on an F-2500 fluorescence spectrophotometer (HITACHI, Tokyo). All samples were dissolved in the mixture of water and methanol (85:15, v/v) with the curcumin equivalent concentration at 5 μg/ml. The excitation wavelength was 420 nm and the emission spectra were recorded from 450 nm to 700 nm. The excitation and emission slit width were the same at 10 nm.

Micelle Preparation and Drug Loading

The dialysis method was used to prepare three types of placebo and drug-loaded micelles: mPEG-PLA, mPEG-PLA-Cur, and mPEG-PLA-Tris-Cur (18). Briefly, 30 mg polymer dissolved in 10 mL THF with excess curcumin was dialyzed against 2 L of ultrapure water using a regenerated cellulose membrane tube (MWCO 2 kD); the dialysis medium was replaced every 6 h. After 24 h the dialyzed solution was centrifuged for 10 min (1,000×*g*), filtered through a microfilter with a membrane pore size of 0.45 μm, and then lyophilized to get the drug-loaded micelles. Placebo micelles without encapsulated drug were produced using the same protocol without free curcumin in the THF solution. To determine the drug content in both placebo and drug-encapsulated micelles, certain amount of micelles (10 mg) were dissolved in methanol and the drug concentration was quantified by a UV–vis spectrophotometer at a wavelength of 426 nm (UV-2450, Shimadzu, Japan).

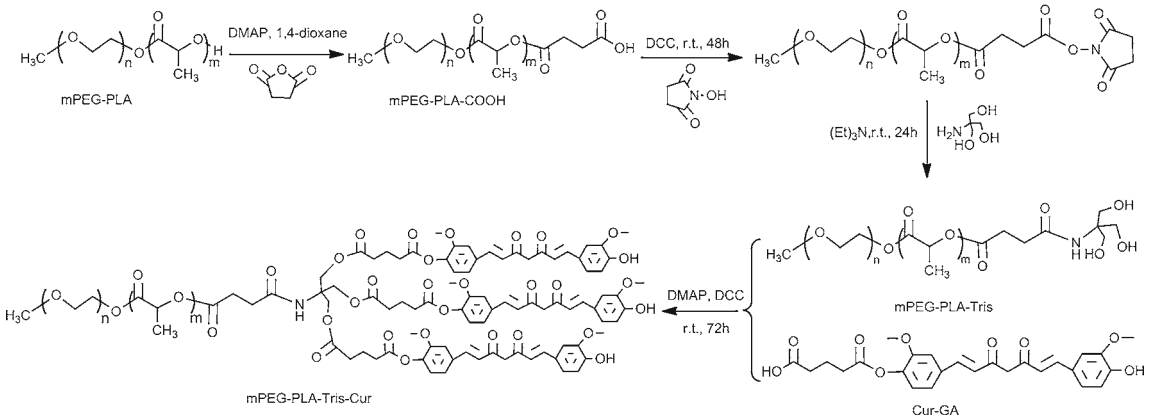

Scheme 2 The synthesis route of mPEG-PLA-Tris-Cur. The structure of mPEG-PLA-Tris-Cur was only illustrative and as a consequence of steric effect only two curcumin molecules could be conjugated to the polymer backbone.

The drug content was calculated by dividing the drug mass by the total amount of micelles.

Characterization of Polymers and Micelles

^{1}H NMR spectra of the synthesized polymer, polymer-drug conjugate and relevant intermediate products were recorded using a 400 MHz Bruker AVANCE III-400 spectrometer (Ettlingen, Germany) in chloroform-d ($CDCl_3$) (d= 7.28 ppm) as the solvent and tetramethylsilane (TMS) as a reference standard for chemical shifts. The weight average molecular weight (M_w) and number average molecular weights (M_n) of the synthesized products were determined by gel permeation chromatography (GPC, polystyrene standards, Agilent, USA) at 30°C; THF was used as the eluent with a flow rate of 1 mL/min. The average grafted curcumin number per conjugate molecule (G_{cur}) was determined using the following Eqs. 1, 2 for mPEG-PLA-Cur and mPEG-PLA-Tris-Cur, respectively:

$$G_{cur} = \frac{M_w(Conjugate) - M_w(mPEG - PLA) + M_w(H_2O)}{M_w(Cur - GA)} \quad (1)$$

$$G_{cur} = \frac{M_w(Conjugate) - M_w(mPEG - PLA - Tris) + 3 \times M_w(H_2O)}{M_w(Cur - GA)} \quad (2)$$

where $M_w(Conjugate)$, $M_w(mPEG\text{-}PLA)$, $M_w(mPEG\text{-}PLA\text{-}Tris)$, $M_w(Cur\text{-}GA)$, *and* $M_w(H_2O)$ are the molecular weight of polymer-drug conjugate, mPEG-PLA, mPEG-PLA-Tris, Cur-GA, and water, respectively.

Both placebo and curcumin-encapsulated micelles were characterized in terms of morphology, size, surface charge, and critical micelle concentration (CMC). The morphology of the micelles was observed via transmission electron microscopy (Tecnai G2 F20, FEI). One drop of diluted aqueous solution of micelles was placed onto a collodion support on copper grids and allowed to air-dry at ambient temperature prior to image-taking. The hydrodynamic size and zeta potential of both placebo and drug-encapsulated micelles were determined in triplicate at 25°C by a Zetasizer Nano ZS (Malvern Instruments).

The CMC of micelles was determined by a fluorescence spectrophotometer (970CRT, Jingke, Shanghai, China) using pyrene as the fluorescence probe (25,29). Micelle aqueous solutions ranging from 0.4 to 400 μg/mL were equilibrated with a fixed pyrene concentration of 2×10^{-9} μM. The emission spectrum was recorded from 350 to 450 nm with an excitation wavelength of 330 nm. The intensity ratio (I_{375}/I_{373}) of pyrene fluorescence bands at 375 nm and 373 nm was plotted against the logarithm of micelle concentration; the CMC was determined by taking the flexion point of the sigmoidal curve.

In Vitro Drug Release

The profiles of *in vitro* curcumin release from polymer-drug conjugate micelles were investigated at 37°C in phosphate buffered saline (PBS) (0.01 M, pH 7.4) containing 5% (w/v) sodium dodecyl sulphate (SDS) to maintain the sink condition (n=3). The unmodified curcumin was used as the control. Individually calibrated upright Franz cells were employed for the release experiments; the cells have an average receptor volume of 15 ml and an average surface area of 2 cm^2. The regenerated cellulose membrane (molecular weight cut-off: 2,000 Da) was used to separate the donor and receptor compartment. The membrane was cut to fit the Franz cells, mounted and sealed between the two chambers of the cells with a magnetic flea in the receptor compartment. The cells were left to equilibrate for 1 h prior to application of donor phase (2 ml conjugate micelles or unmodified curcumin in PBS+SDS). At pre-determined

intervals of time, 0.5 ml sample was withdrawn from the receptor compartment and the same amount of fresh release medium was added. The sample was then assayed for drug content by HPLC and the cumulative amount of released curcumin was plotted against the time. At the end of experiments, the drug residue in the donor phase was cleared with the release medium followed by the drug content analysis to calculate the total drug recovery.

Stability Analysis

The physical stability of micelles and chemical stability of curcumin were investigated based on a previously published method with minor modification (30). The micelle samples were maintained in physiological pH (PBS, 0.01 M, pH 7.4) at 5°C. At pre-determined time point (10, 20 and 30 days), the samples were analysed in terms of hydrodynamic diameter, zeta potential, and curcumin content. All the experiments were performed in triplicate.

Hemolytic Toxicity of Micelles

Hemolytic studies were performed using human erythrocyte suspension *in vitro* (31). The human blood collected from Huang-Hua Orthopaedic Hospital (China) was centrifuged at 800×*g* for 10 min and the supernatant was removed. The red blood cells (RBC) collected at the bottom of centrifuge tube were washed by normal saline (0.9%, w/v) until a clear, colourless supernatant was obtained, and then re-suspended in normal saline (2%, w/v) for further hemolytic investigations. The RBC suspension (2 mL) was mixed with either controls or micelle samples (2 mL) followed by incubation at 37°C for 4 h. Normal saline and double distilled water were used as negative (0% hemolysis) and positive (100% hemolysis) control, respectively. Three types of placebo or drug-encapsulated micelles (mPEG-PLA, mPEG-PLA-Cur, and mPEG-PLA-Tris-Cur) at differing concentration (10–500 μg/ml) in normal saline were evaluated. After incubation, the samples were centrifuged at 800×*g* for 15 min; the supernatant were analysed spectrophotometrically (UV-2450, Shimadzu, Japan) against normal saline at 545 nm. The degree of hemolysis was calculated by the following equation:

$$Hemolysis(\%) = \frac{A_s - A_0}{A_{100} - A_0} \times 100 \quad (3)$$

where A_s, A_0, and A_{100} are the absorbance of micelle sample, negative and positive control, respectively.

Cytotoxicity Assay

The cytotoxicity of polymer-curcumin conjugate micelles was examined by a standard (3-(4,5-Dimethylthiazol-2-yl)-2,5-diphenyltetrazolium bromide) (MTT) assay in HepG2 cells. Briefly, HepG2 cells grown in F-12 K medium containing 10% fetal bovine serum were seeded onto 96-well plates (4,000 cells/well) and incubated at 37°C. After 24 h, the culture medium was replaced with 200 μl fresh one containing different concentration of curcumin (5–50 μg/ml). After 48 h, the cells were washed with PBS five times followed by adding 200 μl MTT-containing culture medium (0.5 mg/ml). After 6 h, the medium was removed and the cells were washed by PBS three times. Afterwards, 150 μl DMSO was added to dissolve the formazan prior to spectrophotometric measurement at 490 nm. Pure curcumin as control was dissolved in dimethyl sulfoxide and diluted with culture medium for MTT assay. The half maximal inhibitory concentration (IC_{50}) of different micelles were calculated using Origin software (OriginLab, Northampton, MA) (n=5).

Cellular Uptake of Micelles

HepG2 cells maintained in DMEM supplemented with 10% fetal bovine serum and 100 U/mL penicillin/streptomycin were cultured at 37°C and 5% CO_2. The cells were seeded in 35 mm culture plates (MatTek, USA) at a seeding density of 2.5×10^4 cells per well in 1 mL of growth medium. The cells were incubated for 24 h, and then the growth medium was replaced with the fresh one containing either placebo or drug-encapsulated micelles. The curcumin content was set at 50 μg/mL and pure drug dissolved in dimethylsulfoxide was used as a control. After incubation for 6 h, the cells were washed with PBS three times. Taking advantage of the intrinsic green fluorescence of curcumin, the confocal laser scanning microscope (CLSM) (LSM 710, Zeiss, Germany) equipped with a multi-Argon laser using FITC filter (excitation at 488 nm) was employed to analyse the localization of curcumin in HepG2 cells.

Statistical Analysis

Statistical analysis of data was performed using SPSS v.18 and a statistically significant difference was determined at a minimal level of significance of 0.05. Data were analysed using one way ANOVA with Turkey's post-hoc test.

RESULTS & DISCUSSION

Synthesis and Characterization of Polymer-Drug Conjugate

Curcumin was slightly modified with one phenolic hydroxyl group of the drug being transformed to the carboxyl group facilitating the conjugation with polymer. The generation of Cur-GA was proved by proton signal of the methylene

group from glutaric acid (Figure S1). In addition, obvious splits of the chemical shifts of both aromatic and non-aromatic methine protons in the drug moiety of Cur-GA were observed. The chemical shift of methoxyl proton in unmodified curcumin appeared as a singlet (3.90 ppm), whist it split into two peaks at 3.90 and 3.97 ppm after modification by GA. All these demonstrated the generation of Cur-GA.

mPEG-PLA was synthesized through ring-opening polymerization of L-lactide with mPEG as the macroinitiator in the presence of stannous octanoate (Scheme 1). The M_n of the copolymer was determined by ^{1}H NMR to be 3,517 via comparing the integral area of the peaks at 5.19 ppm (OC*H*CH$_3$CO in PLA) and 3.66 ppm (CH_2CH_2O in mPEG) (Figure S2), which corresponded with the molecular weight determined by GPC (Table I). Carboxyl group-terminated mPEG-PLA was also confirmed by ^{1}H NMR analysis (2.72 ppm, -COCH_2CH_2COOH) (Figure S2). Tris was employed to triplicate the terminal hydroxyl group of mPEG-PLA-COOH enabling the conjugation of multiple drug molecules to the polymer backbone. The presence of proton signal of –NH- group at 8.03 ppm verified the successful synthesis of mPEG-PLA-Tris (Figure S2).

Two types of polymer-drug conjugates, i.e. mPEG-PLA-Cur and mPEG-PLA-Tris-Cur were generated via the formation of ester bonds between Cur-GA and the polymer (mPEG-PLA-COOH or mPEG-PLA-Tris). The formation of these conjugates was proved by the ^{1}H NMR spectra that showed the proton resonance peaks corresponding to both the parent drug and the polymers (Fig. 2). The presence of multiple proton resonance peaks of curcumin (5.88–7.77 ppm) together with the distinctive –OCH_3 protons (3.40 ppm) and -CH_2 protons (3.66 ppm) of mPEG, and the characteristic –CH_3 protons (1.61 ppm) and –C*H* proton (5.19 ppm) of PLA confirmed the formation of mPEG-PLA-Cur conjugate (Fig. 2a). Similarly, apart from the above characteristic peaks, the proton resonance at 8.16 ppm that corresponded to the –NH group verified the successful synthesis of mPEG-PLA-Tris-Cur (Fig. 2b). The fluorescence spectra of mPEG-PLA-Cur and mPEG-PLA-Tris-Cur also proved the successful synthesis (Fig. 3). Curcumin shows intrinsic fluorescent properties. The hypsochromic shift (to lower wavelength) of polymer-curcumin conjugate compared to pure curcumin demonstrated the conjugation between the polymer and the drug. The polymer-drug conjugates were also validated by GPC analysis (Table I). The gradual increase of molecular weight (M_w) of both types of conjugates compared to mPEG-PLA further proved the conjugation between curcumin and the polymer. Via comparing the M_w difference of conjugates and corresponding polymer backbone, the average molecules of curcumin grafted to the polymer was calculated to be 1.0 (mPEG-PLA-Cur) and 2.0 (mPEG-PLA-Tris-Cur), respectively. The incapability to conjugate three curcumin molecules to the polymer backbone via the Tris linker was assumed as a result of the steric hindrance. Due to the polydisperse nature of polymer, both types of polymer-curcumin conjugates displayed a polydispersity index of ca. 1.2, which is comparable to that of mPEG-PLA (Table I).

Table I The Molecular Weight and Polydispersity Index (PI) of Three Types of Conjugates: mPEG-PLA, mPEG-PLA-Cur, and mPEG-PLA-Tris-Cur. mPEG, PLA, Tris, and Cur signify methoxy poly(ethylene glycol), poly(lactic acid), tris (hydroxymethyl)aminomethane, and curcumin, respectively

Conjugate Sample	M_n	M_w	PI	G_{cur}
mPEG-PLA	3242	3719	1.15	—
mPEG-PLA-Cur	3439	4135	1.20	1.0
mPEG-PLA-Tris-Cur	4040	4728	1.17	2.0

The number average molecular weight (M_n) and weight average molecular weight (M_w) were obtained from gel permeation chromatography analysis. G_{cur} denote the average grafted curcumin per conjugate molecule.

Micelle Generation and Characterization

Three types of micelles were generated in aqueous media by the self-assembly of amphiphilic mPEG-PLA, mPEG-PLA-Cur and mPEG-PLA-Tris-Cur. The driving force of micelle formation is the decrease of free energy in the system as a consequence of the removal of hydrophobic moiety away from the aqueous environment forming the micelle core that is stabilized by the hydrophilic moiety exposed into water (32). PEG was selected as the hydrophilic block because it presents many unique properties including low immunogenicity and toxicity, high solubility in water and many organic solvents, low cost, and superior chain flexibility (33). Additionally, PEG has been approved by FDA for human use. The reason to select PLA as the hydrophobic block is due to the biodegradability and biocompatibility of polyesters that have been widely used in drug delivery field. Furthermore, the molecular weight of PLA can be readily regulated to control the length of the hydrophobic block, and thus the size of micelles.

Irrespective of the micelle type, the sizes of both placebo and curcumin-encapsulated micelles were within 100 nm (Table II). Micelles made of polymer-drug conjugate were significantly larger than mPEG-PLA micelles ($p<0.05$). It is assumed that the presence of curcumin in the hydrophobic moiety modifies the driving force of micelle formation. In addition, the conjugate architecture might bring about a crowding effect resulting in bigger micelles. The micelle morphology was revealed by TEM (Fig. 4). All types of micelles with or without encapsulated drug were spherical and well-separated without aggregation. The approximate diameter of these micelles was within 100 nm, which coincided with the hydrodynamic size. Previous investigation showed that the longer hydrophilic block compared to the hydrophobic block aided the formation of amphiphilic polymer micelles;

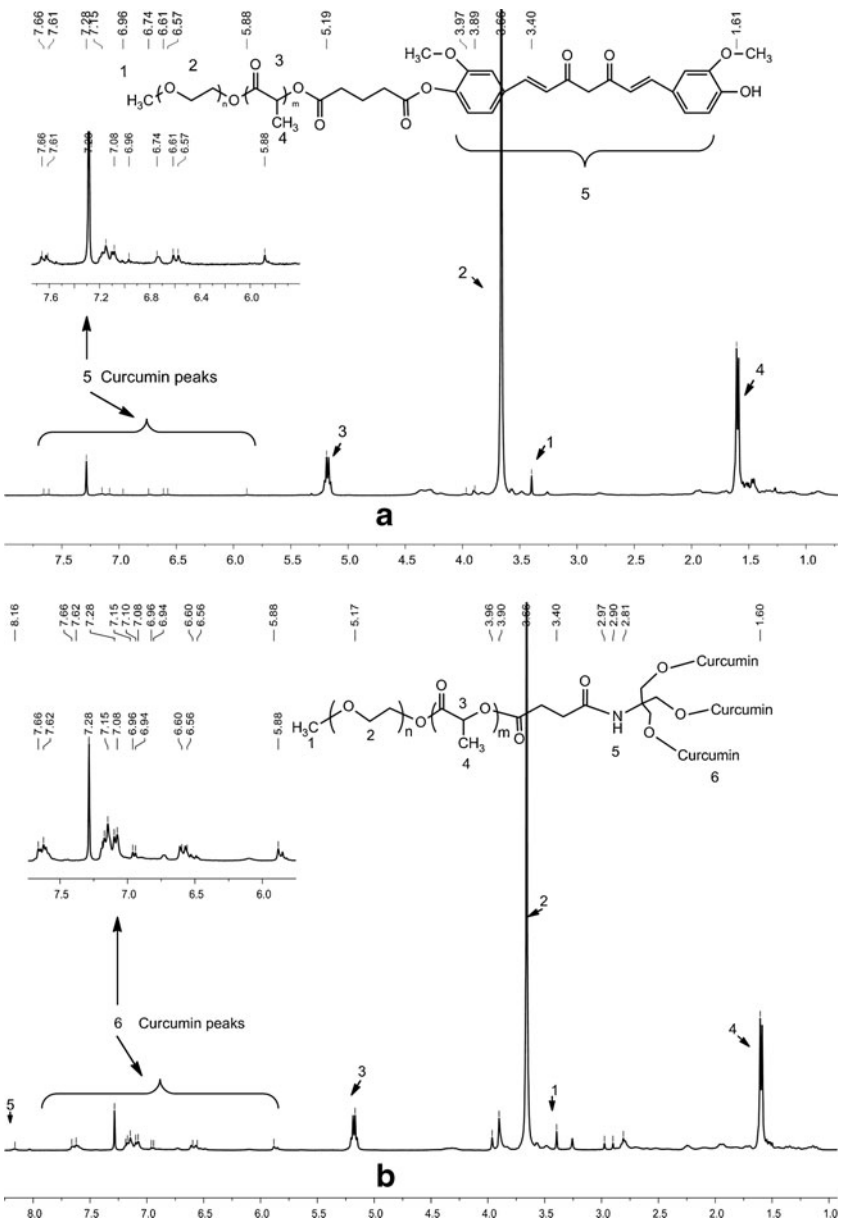

Fig. 2 Qualitative ^{1}H NMR spectra showing the characteristic proton resonance peaks of (**a**) mPEG-PLA-Cur and (**b**) mPEG-PLA-Tris-Cur. mPEG, PLA, Tris, and Cur signify methoxy poly(ethylene glycol), poly(lactic acid), tris(hydroxymethyl)aminomethane, and curcumin, respectively. The ideal structure of mPEG-PLA-Tris-Cur was presented here and practically due to steric effect only two curcumin molecules could be conjugated to the polymer backbone.

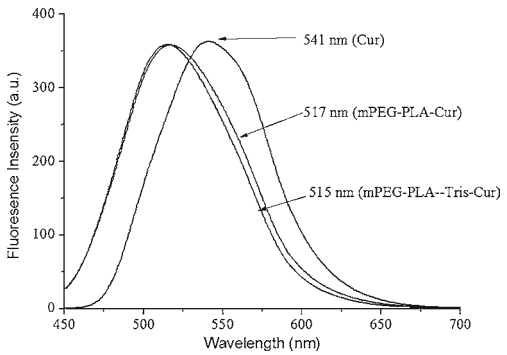

Fig. 3 The fluorescence spectra of curcumin (Cur), mPEG-PLA-Cur, and mPEG-PLA-Tris-Cur. mPEG, PLA, and Tris signify methoxy poly(ethylene glycol), poly(lactic acid), and tris(hydroxymethyl)aminomethane, respectively. The drug concentration was fixed at 5 μg/ml and the solvent was a mixture of water (85%, v/v) and methanol (15%, v/v).

nevertheless, too long hydrophilic block generated individual water-soluble molecules and too long hydrophobic block lead to the formation of non-sphere structures such as rods and lamellae (34,35). In this study, we chose low molecular weight mPEG (ca. 2 kD) and manipulated the length of hydrophobic block less than that of mPEG during PLA synthesis, which successfully generated spherical micelles within nano-range.

Zeta potential as an index denotes the charge difference between the dense layers of ions absorbed onto the micelle surface and the bulk of the dispersing medium. PLA particles have been shown to exhibit a negative zeta potential ca. −50 mV due to the presence of terminal carboxyl group at the particle surface (36). The decrease of zeta potential of mPEG-PLA at ca. −6 mV was attributed to the surface shielding effect of non-ionic PEG that offset the negative

Table II The Hydrodynamic Size, Zeta Potential, Loading of Three Types of Micelles (placebo and drug-encapsulated): mPEG-PLA, mPEG-PLA-Cur, and mPEG-PLA-Tris-Cur Within 1 month at 5°C

Micelle Type	Day	Hydrodynamic diameter (nm)	Zeta potential (mV)	Drug loading (%, w/w)
mPEG-PLA (placebo)	0	56.4 ± 0.9	-5.4 ± 0.6	–
	10	61.3 ± 1.3	-4.4 ± 0.8	–
	20	64.3 ± 1.8	-5.1 ± 1.0	–
	30	65.8 ± 2.1	-4.6 ± 0.8	–
mPEG-PLA (drug-encapsulated)	0	60.3 ± 3.2	-8.2 ± 1.2	2.3 ± 0.6
	10	67.7 ± 4.2	-5.2 ± 0.9	2.0 ± 0.9
	20	71.7 ± 1.2	-6.2 ± 0.5	1.7 ± 0.6
	30	73.7 ± 1.6	-5.8 ± 0.4	1.6 ± 0.9
mPEG-PLA-Cur (placebo)	0	74.1 ± 1.2	-18.4 ± 1.1	3.6 ± 0.4
	10	73.9 ± 1.6	-17.4 ± 0.7	3.4 ± 0.5
	20	75.1 ± 0.9	-16.4 ± 0.3	3.2 ± 0.7
	30	75.9 ± 0.6	-17.5 ± 0.8	3.2 ± 0.9
mPEG-PLA-Cur (drug-encapsulated)	0	80.5 ± 1.4	-16.7 ± 0.9	8.5 ± 0.9
	10	84.3 ± 2.3	-17.7 ± 1.5	8.1 ± 0.6
	20	87.5 ± 1.1	-17.1 ± 0.6	7.8 ± 0.6
	30	89.5 ± 1.3	-18.1 ± 0.5	7.5 ± 1.6
mPEG-PLA-Tirs-Cur (placebo)	0	79.6 ± 2.1	-18.9 ± 1.7	9.8 ± 0.7
	10	82.6 ± 1.4	-17.9 ± 2.3	9.5 ± 0.8
	20	84.5 ± 0.8	-15.9 ± 1.3	9.4 ± 0.6
	30	84.9 ± 1.1	-16.3 ± 1.1	9.4 ± 1.1
mPEG-PLA-Tirs-Cur (drug-encapsulated)	0	102.8 ± 1.2	-16.5 ± 2.1	18.5 ± 1.3
	10	99.6 ± 3.2	-17.5 ± 1.1	17.6 ± 0.9
	20	101.6 ± 2.8	-18.3 ± 1.4	17.3 ± 1.3
	30	100.8 ± 1.8	-17.6 ± 0.8	16.9 ± 0.7

mPEG, PLA, Tris, and Cur signify methoxy poly(ethylene glycol), poly(lactic acid), tris(hydroxymethyl)aminomethane, and curcumin, respectively (n=3).

charge of the PLA segment and shifted the shear plane of the diffusion layer farther away from micelle surface (Table II). Such effect has been observed in other previous investigations (37,38). Compared to mPEG-PLA, a significantly increase ($p<0.05$) in the absolute values of zeta potential of the polymer-drug conjugate micelles (mPEG-PLA-Cur and mPEG-PLA-Tris-Cur) could be related to the conjugation of Cur to PLA that not only lengthened the hydrophobic block, but also offered the block multiple carboxyl groups (Table II). A previous independent study produced PEG-Cur conjugate micelles with a zeta potential of ca. −20 mV, which agreed with our results (5). It has been demonstrated that increasing PEG length (i.e. >5 kD) could effectively shield the surface charge of particles because of the shift of the hydrodynamic phase of shear to much greater distance outwards from the particle surface at the cost of remarkable increase of micelle size (39). However, in current study the presence of a negative surface for polymer-curcumin conjugate micelles would help to stabilize these micelles via both the steric and electrostatic mechanisms.

One of the key concerns for micellar drug delivery systems is the *in vivo* stability at a high dilution upon parenteral administration (25). The CMC is a good index to denote the thermodynamic stability of micelles upon dilution; the lower the CMC, the more stable the micelles. In this study, pyrene was employed as a probe for CMC determination by fluorescence spectroscopy. When the probe translocated from the aqueous medium to the micelle core, its fluorescent properties would change accordingly. The CMC of mPEG-PLA, mPEG-PLA-Cur, and mPEG-PLA-Tris-Cur were 27.4 ± 0.8, 7.8 ± 1.3, and 2.3 ± 0.4 μg/mL, respectively (Fig. 5). The CMC of polymer-drug conjugate micelles was significantly lower compared to that of mPEG-PLA ($p<0.05$), indicating a radically improved stability of conjugate micelles. Such results can be explained by the hydrophobicity increase of the entire hydrophobic block of micelles after curcumin conjugation because of the hydrophobic nature of curcumin (log *P* 3.2), which was consistent with other previous studies (25,40). However, the CMC of PEG-Cur micelles without PLA segment was much higher at 50 μg/mL (5), suggesting that the low CMC of conjugate micelles in current study benefited from the coexistence of both PLA and Cur. The short PEG segment also made a contribution to the low CMC of conjugate micelles since the increase of the hydrophilic block would result in an increase of CMC (41). From the viewpoint of the driving force of micelle formation, conjugates

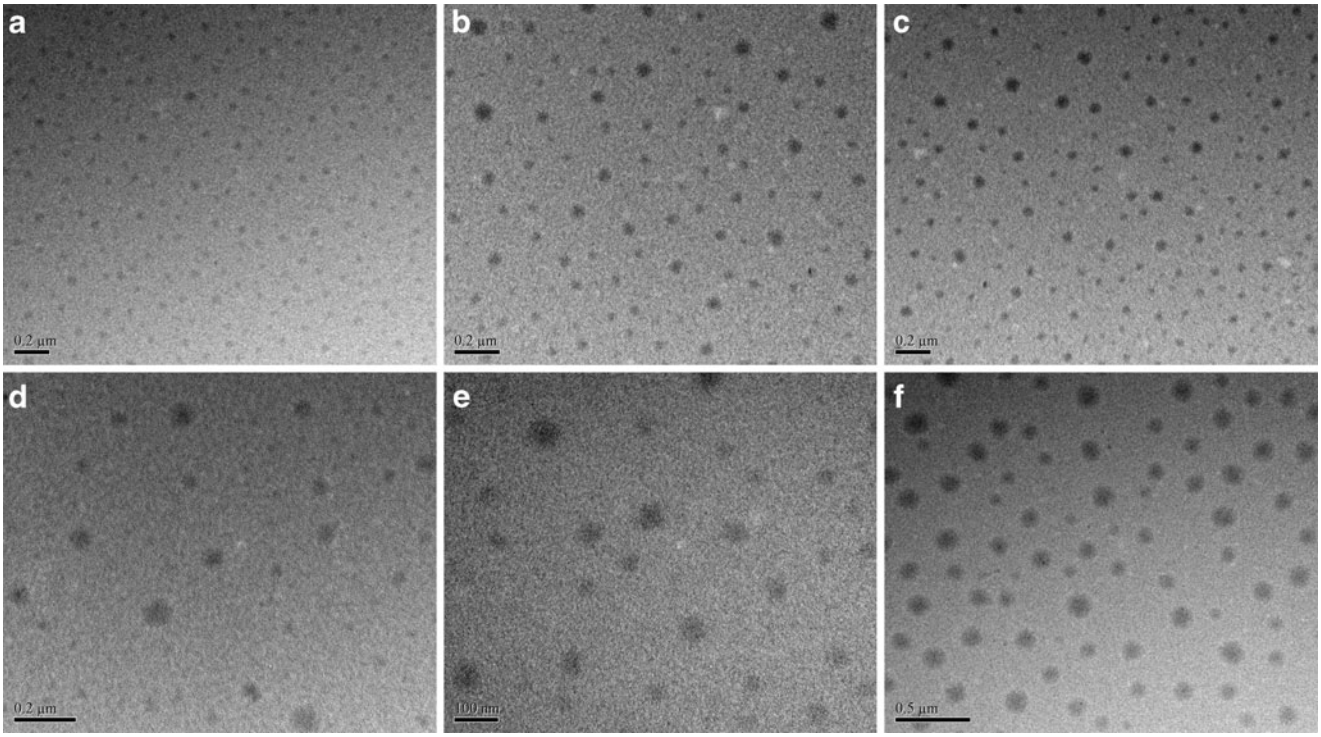

Fig. 4 Transmission electron microscopy (TEM) analysis of placebo (**a**–**c**) and drug-encapsulated (**d**–**f**) amphiphilic copolymer micelles: mPEG-PLA (**a,d**), mPEG-PLA-Cur (**b,e**), mPEG-PLA-Tris-Cur (**c,f**). mPEG, PLA, Tris, and Cur signify methoxy poly(ethylene glycol), poly(lactic acid), tris(hydroxymethyl)aminomethane, and curcumin, respectively.

with a more hydrophobic block are easier to self-assemble for the decrease of system free energy accounting for a low CMC. Interestingly, linking more than one curcumin molecules to the PLA moiety (i.e. mPEG-PLA-Tris-Cur) further increased the hydrophobicity of the micelle hydrophobic block compared to that containing only one drug (i.e. mPEG-PLA-Cur). This result implied that using the Tris linker to conjugate multiple hydrophobic drugs to the backbone of amphiphilic copolymers was an efficient approach to enhance micelle stability. The generation of biodegradable polymer-drug conjugate micelles with very low CMC was valuable in formulating hydrophobic active agents as the use of large quantity of surfactants or other solubilizers traditionally can be avoided or minimized to reduce the toxicity and other side-effects, and to prevent drug precipitation (premature burst release) upon dilution with the physiological fluids.

Drug Loading and Release

The curcumin loading in placebo mPEG-PLA-Cur and mPEG-PLA-Tris-Cur micelles was $3.6 \pm 0.4\%$ and $9.8 \pm 0.7\%$, respectively; after drug encapsulation the curcumin content increased to $8.5 \pm 0.9\%$ and $18.5 \pm 1.3\%$ correspondingly that was an extensive increase compared to that

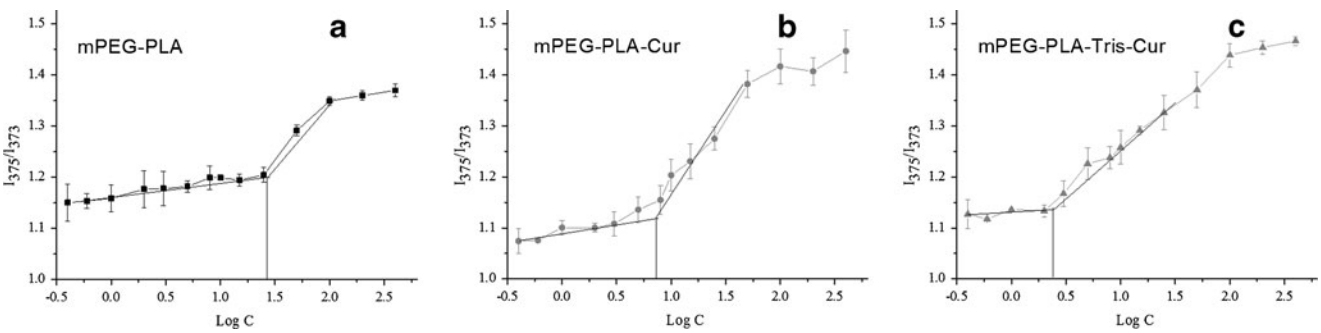

Fig. 5 Critical micelle concentration (CMC) of three types of placebo amphiphilic copolymer micelles: (**a**) mPEG-PLA, (**b**) mPEG-PLA-Cur, and (**c**) mPEG-PLA-Tris-Cur. mPEG, PLA, Tris, and Cur signify methoxy poly(ethylene glycol), poly(lactic acid), tris(hydroxymethyl)aminomethane, and curcumin, respectively. Intensity ratio (375/373 nm) from pyrene emission spectra was plotted against the logarithm of micelle concentration; the CMC was obtained by taking the flexion point of the sigmoidal curve.

of mPEG-PLA micelles at 2.3±0.6% (Table II). After curcumin encapsulation, the size of conjugate micelles increased significantly compared to the placebo ones ($p<0.05$) (Table II), but still remained within 100 nm, which can avoid the removal in systemic circulation by MPS and take the advantage of EPR effect for passively targeting curcumin to the pathological sites. The extent of size increase also differed greatly upon curcumin loading and the size growth was ca. 4 nm, 6 nm, and 20 nm for mPEG-PLA, mPEG-PLA-Cur, and mPEG-PLA-Tris-Cur, respectively, which was caused by the expansion of micelle core and concurred with the differing loading capability of three types of micelles. Previous mathematical simulation of the solubilisation process of amphiphilic polymeric micelles indicated that the initial drug solubilisation began via the displacement of aqueous medium from the micelle core followed by drug accumulation in the core centre, which forced the hydrophobic block away from the core and thus lead to the expansion of micelles (34,42). The conjugation of curcumin to the hydrophobic moiety of micelles has three roles: (a) improve drug loading directly, (b) enhance the interaction between the hydrophobic blocks, and (c) increase the affinity between the encapsulated drug and the micelle core. The presence of several hydrogen donor and receptor in curcumin could facilitate such interactions via hydrogen bonding and thus help to increase the encapsulated drug content through an indirect way. In addition, the conjugation increased the length of hydrophobic block producing a bigger core size (Table II) with boosted ability for curcumin encapsulation. This was evidenced by the superior loading capability of both types of conjugate micelles. The hydrogen-bonding-enhanced loading of hydrophobic doxorubicin in urea-containing amphiphilic copolymer micelles was reported (43). Likewise, a very recent study employed cholesterol to modify the hydrophobic segment of the amphiphilic copolymer micelles and achieved an enhanced loading of paclitaxel (44). Upon administration, the encapsulated drug would be released by diffusion, whilst the conjugated form would be freed via the hydrolysis of ester bond between PLA and curcumin.

The *in vitro* drug release study showed that mPEG-PLA-Cur and mPEG-PLA-Tris-Cur conjugate micelles exhibited a sustained release profile compared to the unmodified curcumin (Fig. 6). The drug release profiles of mPEG-PLA-Cur and mPEG-PLA-Tris-Cur were analogous and both levelled off after 12 h, which was because the release was largely controlled by the hydrolysis process. However, due to the instability of curcumin at basic condition with elevated temperature, the release experiment was mixed up with drug degradation process. It has been reported previously that when curcumin was incubated in PBS (0.1 M, pH 7.2) at 37°C, the majority of the drug decomposed within a few hours (45). The mass balance study also proved this in current study and the total drug recovery after 60 h was ca. 50% for both the control and micelles.

Stability and Cytotoxicity Studies

The physical stability of conjugate micelles was analysed in terms of hydrodynamic diameter and zeta potential (Table II). At the end of 1 month these micelles maintained colloidal stability and no aggregation was observed. The chemical stability of curcumin in these micelles was assessed by monitoring the drug content at different time points. For mPEG-PLA-Cur and mPEG-PLA-Tris-Cur micelles without encapsulated drug (placebo), there was no significant change of curcumin content within 1 month. However, for all the other micelles containing encapsulated curcumin, the drug content slightly reduced. This can be explained by the fact that the encapsulated drug may diffuse out of the micelles and then degraded due to the inherent instability of curcumin. Such data also verified that upon conjugation with polymer the chemical stability of curcumin can be enhanced.

The cytotoxicity of curcumin in different micelles was evaluated using IC_{50} in HepG2 cell lines (Table III). There was no significant difference between the IC_{50} value of pure curcumin and that of three types of drug-encapsulated micelles, i.e. mPEG-PLA/Cur, mPEG-PLA-Cur/Cur, and mPEG-PLA-Tris-Cur/Cur. Nevertheless, the IC_{50} of mPEG-PLA-Cur (42.8±1.5 μg/ml) and mPEG-PLA-Tris-Cur (39.3±4.9 μg/ml) was significantly larger compared to their counterpart mPEG-PLA-Cur/Cur (28.3±6.1 μg/ml) and mPEG-PLA-Tris-Cur/Cur (22.3±7.0 μg/ml), respectively. Such divergence might be a consequence of the difference of drug release rate from micelles inside the cells.

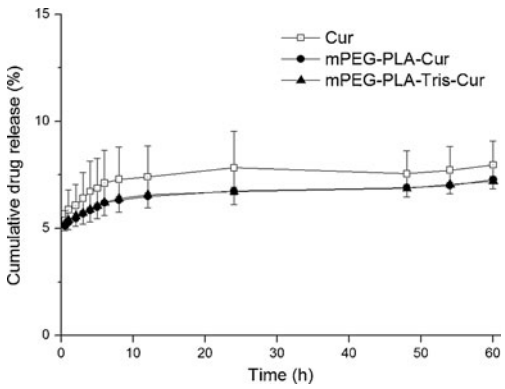

Fig. 6 *In vitro* release profile of curcumin (Cur) from different micelles and unmodified Cur at 37°C in PBS (pH 7.4). mPEG, PLA, and Tris signify methoxy poly(ethylene glycol), poly(lactic acid), and tris(hydroxymethyl)aminomethane, respectively. Data were expressed as mean ± standard deviation ($n=3$).

Table III The Half Maximal Inhibitory Concentration (IC_{50}) of Curcumin, Polymer-Curcumin Conjugate Micelles (mPEG-PLA-Cur and mPEG-PLA-Tris-Cur), and Curcumin-Encapsulated Micelles (mPEG-PLA/Cur, mPEG-PLA-Cur/Cur, and mPEG-PLA-Tris-Cur/Cur) in the Human Hepatocellular Carcinoma Cell Line (HepG2)

Sample	IC_{50} (μg/ml)
Cur	27.5 ± 5.7
mPEG-PLA/Cur	29.1 ± 10.1
mPEG-PLA-Cur	42.8 ± 1.5
mPEG-PLA-Cur/Cur	28.3 ± 6.1
mPEG-PLA-Tris-Cur	39.3 ± 4.9
mPEG-PLA-Tris-Cur/Cur	22.3 ± 7.0

mPEG, PLA, Tris, and Cur signify methoxy poly(ethylene glycol), poly(lactic acid), tris(hydroxymethyl)aminomethane, and curcumin, respectively. Data were presented as mean ± standard deviation (n=5).

Hemolytic Toxicity and Cellular Update

RBC lysis is a simple method to investigate the micelle-cell membrane interaction. mPEG-PLA, mPEG-PLA-Cur, and mPEG-PLA-Tris-Cur micelles in current study all exhibited no sign of hemolysis at the concentration up to 500 μg/ml (the hemolysis degree less than 2%) indicating the superb hemocompatibility of these copolymer micelles. The shielding effect of PEG moiety and the absence of cationic terminal group that was known to destabilize the negatively charged RBC membrane and induce cell lysis were the reasons of such low hemolytic toxicity, which accorded well with previous investigations on the hemolytic activity of PEG-polyester copolymer micelles and other types of curcumin-loaded nanocarriers (46,47).

The intrinsic fluorescence of curcumin was employed to study the internalization of both placebo and drug-encapsulated micelles into HepG2 cells by CLSM without the use of additional probes (Fig. 7). When treating the cells with placebo mPEG-PLA micelles, no fluorescence was detected; however, curcumin-encapsulated mPEG-PLA micelles produced noticeable fluorescence in the cytoplasm of cells. The major difference between the cellular uptake of free and micelle-associated (either conjugated or encapsulated) curcumin was that the former located both in the cytoplasm and nucleus, whilst the latter resided primarily in the cytoplasmic compartment without marked nuclear localization, indicating different internalization mechanisms for both types of curcumin. Similar results were reported using the PEG-polyester micelles and such micelles were often internalized by endocytosis that was time- and concentration-dependent (47,48). Once engulfed by the plasma membrane, the micelles are transported by endosomes and later lysosomes; the acidic endocytic compartments and the presence of large collections of hydrolases facilitate the cleavage of the ester linkage between curcumin and the polymers (49). The release of lactic acid caused by

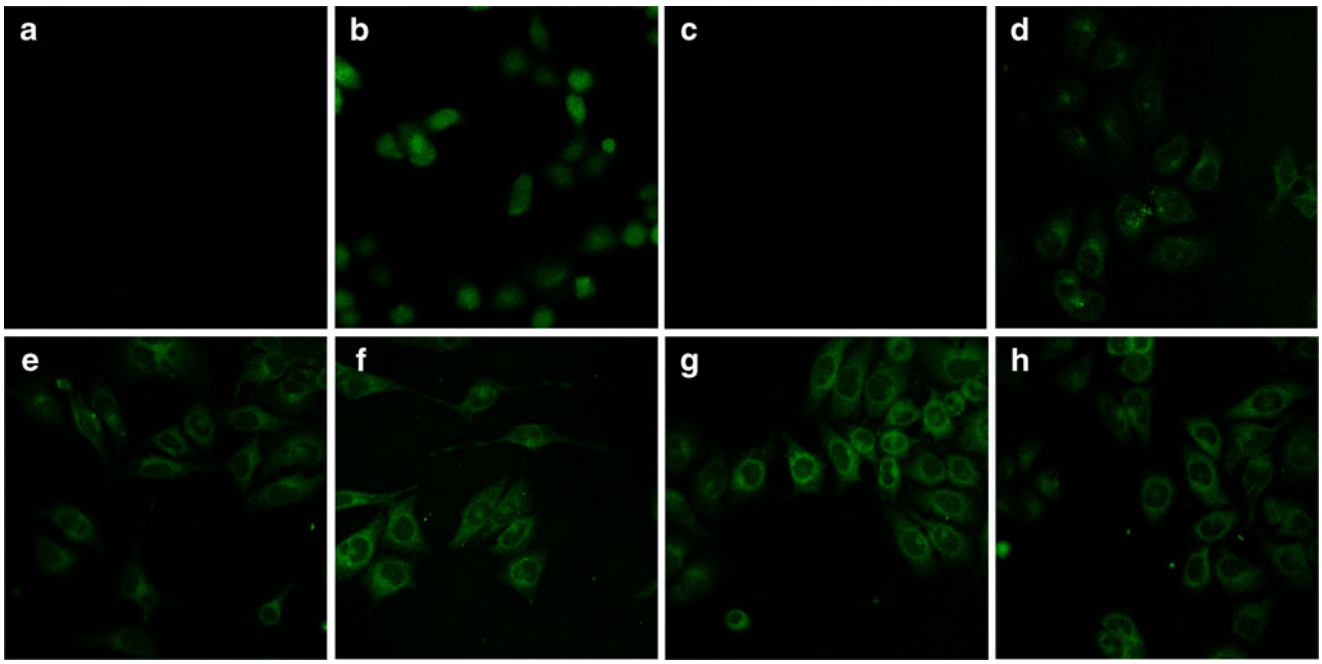

Fig. 7 Internalization of free curcumin (Cur) and different types of micelles in the human hepatocellular carcinoma cell line (HepG2). Confocal laser scanning microscope (CLSM) was used for detecting the intrinsic fluorescence of Cur after incubation with either drug-containing micelles or free Cur for 6 h: (**a**) negative control; (**b**) free Cur; (**c**) placebo mPEG-PLA micelles; (**d**) drug-encapsulated mPEG-PLA micelles (mPEG-PLA/Cur); (**e**) placebo mPEG-PLA-Cur micelles; (**f**) drug-encapsulated mPEG-PLA-Cur micelles; (**g**) placebo mPEG-PLA-Tris-Cur micelles; (**h**) drug-encapsulated mPEG-PLA-Tris-Cur micelles. The drug loading information of these micelles was provided in Table II. mPEG, PLA, and Tris signify methoxy poly(ethylene glycol), poly(lactic acid), and tris(hydroxymethyl)aminomethane, respectively.

the degradation of PLA could further lower the environmental pH aiding the release of conjugated curcumin. An excellent model illustrating the difference of cellular internalization of free drug and micelle-incorporated drug was detailed previously (50). The CLSM images of placebo mPEG-PLA-Cur and mPEG-PLA-Tris-Cur manifested that the polymer-drug conjugate micelles could get into the HepG2 cells. Both types of drug-encapsulated conjugate micelles showed higher fluorescence intensity compared to that of mPEG-PLA, which was assumed to be a result of saturation of the endocytic process leading to reduced micelle entry into cells. Since the loading capability of conjugate micelles was much greater than that of mPEG-PLA, the concentration of conjugate micelles was considerably lower than mPEG-PLA micelle concentration at the same drug dose (Table II). It has been reported that the cellular uptake of curcumin-loaded mPEG-polyester micelles is more effective at lower concentrations in pancreatic cancer cells (18). Similar results were also observed in another independent investigation employing different cell lines (16). As expected, the CLSM analysis revealed that the conjugate micelles changed the subcellular distribution of curcumin and greater content of curcumin was internalized with the aid of conjugate micelles compared to free curcumin, which was consistent with previous studies (5,50). Future work will use multiple-labelling approach to selectively visualize the nucleus, micelles, and the plasma membrane for investigating the detailed subcellular distribution of curcumin.

CONCLUSIONS

Biodegradable amphiphilic polymer-drug conjugate micelle approach was employed to enhance the loading and intracellular delivery of low-potency curcumin. The conjugates contain three segments: hydrophilic PEG, hydrophobic PLA, and curcumin. Via the use of Tris linker, more than one drug molecules were linked to PLA via ester bond. All these conjugates self-assemble into spherical micelles with size less than 100 nm. The loading of curcumin in the conjugate micelles reached ca. 20% (w/w) including both the conjugated and encapsulated form, whilst the loading in traditional mPEG-PLA micelles was only ca. 2% (w/w). These novel conjugate micelles showed no hemolytic toxicity, whilst the cytotoxicity of these curcumin-loaded micelles was comparable to pure curcumin as evidenced by IC_{50} determination. The cellular uptake study demonstrated that these carriers could successfully transport the drug to the cytoplasm of HepG2 cells. Such approach can also be utilized for other hydrophobic active chemotherapeutic ingredients containing hydroxyl groups as well as for combinational delivery of multiple anti-cancer agents.

ACKNOWLEDGMENTS AND DISCLOSURES

This work was supported by Tianjin Research Program of Application Foundation and Advanced Technology (11JCZDJC20600; 11JCYBJC10300), National Natural Science Foundation of China (81171478; 31100699), and the Research Fund for the Doctoral Program of Higher Education of China (20110032120077).

The authors of this article have no conflicts of interest to declare.

REFERENCES

1. Shen Y, Jin E, Zhang B, Murphy CJ, Sui M, Zhao J, Wang J, Tang J, Fan M, Van Kirk E, Murdoch WJ. Prodrugs forming high drug loading multifunctional nanocapsules for intracellular cancer drug delivery. J Am Chem Soc. 2010;132(12):4259–65.
2. Ferrari M. Cancer nanotechnology: opportunities and challenges. Nat Rev Cancer. 2005;5(3):161–71.
3. Shin HC, Alani AWG, Cho H, Bae Y, Kolesar JM, Kwon GS. A 3-in-1 Polymeric Micelle nanocontainer for poorly water-soluble drugs. Mol Pharm. 2011;8(4):1257–65.
4. Peer D, Karp JM, Hong S, Farokhzad OC, Margalit R, Langer R. Nanocarriers as an emerging platform for cancer therapy. Nat Nanotechnol. 2007;2(12):751–60.
5. Tang H, Murphy CJ, Zhang B, Shen Y, Sui M, Van Kirk EA, Feng X, Murdoch W. Amphiphilic curcumin conjugate-forming nanoparticles as anticancer prodrug and drug carriers: in vitro and in vivo effects. Nanomedicine (Lond). 2010;5(6):855–65.
6. Tang H, Murphy CJ, Zhang B, Shen Y, Van Kirk EA, Murdoch WJ, Radosz M. Curcumin polymers as anticancer conjugates. Biomaterials. 2010;31(27):7139–49.
7. Lao C, Ruffin M, Normolle D, Heath D, Murray S, Bailey J, Boggs M, Crowell J, Rock C, Brenner D. Dose escalation of a curcuminoid formulation. BMC Complementary Altern Med. 2006;6(1):10.
8. Anand P, Kunnumakkara AB, Newman RA, Aggarwal BB. Bioavailability of curcumin: problems and promises. Mol Pharm. 2007;4(6):807–18.
9. Yallapu MM, Jaggi M, Chauhan SC. Beta-cyclodextrin-curcumin self-assembly enhances curcumin delivery in prostate cancer cells. Colloids Surf B. 2010;79(1):113–25.
10. Anand P, Nair HB, Sung BK, Kunnumakkara AB, Yadav VR, Tekmal RR, Aggarwal BB. Design of curcumin-loaded PLGA nanoparticles formulation with enhanced cellular uptake, and increased bioactivity in vitro and superior bioavailability in vivo. Biochem Pharmacol. 2010;79(3):330–8.
11. Shahani K, Panyam J. Highly loaded, sustained-release microparticles of curcumin for chemoprevention. J Pharm Sci. 2011;100(7):2599–609.
12. Safavy A, Raisch KP, Mantena S, Sanford LL, Sham SW, Krishna NR, Bonner JA. Design and development of water-soluble curcumin conjugates as potential anticancer agents. J Med Chem. 2007;50(24):6284–8.
13. Zhang F, Koh GY, Jeansonne DP, Hollingsworth J, Russo PS, Vicente G, Stout RW, Liu Z. A novel solubility-enhanced curcumin formulation showing stability and maintenance of anticancer activity. J Pharm Sci. 2011;100(7):2778–89.
14. Manju S, Sreenivasan K. Conjugation of curcumin onto hyaluronic acid enhances its aqueous solubility and stability. J Colloid Interface Sci. 2011;359(1):318–25.

15. Manju S, Sreenivasan K. Synthesis and characterization of a cytotoxic cationic polyvinylpyrrolidone-curcumin conjugate. J Pharm Sci. 2011;100(2):504–11.
16. Ma Z, Haddadi A, Molavi O, Lavasanifar A, Lai R, Samuel J. Micelles of poly(ethylene oxide)-b-poly(epsilon-caprolactone) as vehicles for the solubilization, stabilization, and controlled delivery of curcumin. J Biomed Mater Res A. 2008;86(2):300–10.
17. Gou M, Men K, Shi H, Xiang M, Zhang J, Song J, Long J, Wan Y, Luo F, Zhao X, Qian Z. Curcumin-loaded biodegradable polymeric micelles for colon cancer therapy *in vitro* and *in vivo*. Nanoscale. 2011;3(4):1558–67.
18. Mohanty C, Acharya S, Mohanty AK, Dilnawaz F, Sahoo SK. Curcumin-encapsulated MePEG/PCL diblock copolymeric micelles: a novel controlled delivery vehicle for cancer therapy. Nanomedicine (Lond). 2010;5(3):433–49.
19. Pitarresi G, Palumbo FS, Albanese A, Fiorica C, Picone P, Giammona G. Self-assembled amphiphilic hyaluronic acid graft copolymers for targeted release of antitumoral drug. J Drug Target. 2010;18(4):264–76.
20. Sahu A, Bora U, Kasoju N, Goswami P. Synthesis of novel biodegradable and self-assembling methoxy poly(ethylene glycol)-palmitate nanocarrier for curcumin delivery to cancer cells. Acta Biomater. 2008;4(6):1752–61.
21. Li ZB, Kesselman E, Talmon Y, Hillmyer MA, Lodge TP. Multicompartment micelles from ABC miktoarm stars in water. Science. 2004;306(5693):98–101.
22. Yokoyama M, Kwon GS, Okano T, Sakurai Y, Seto T, Kataoka K. Preparation of micelle-forming polymer-drug conjugates. Bioconjugate Chem. 1992;3(4):295–301.
23. Hu X, Jing X. Biodegradable amphiphilic polymer-drug conjugate micelles. Expert Opin Drug Deliv. 2009;6(10):1079–90.
24. Discher DE, Kamien RD. Self-assembly —towards precision micelles. Nature. 2004;430(6999):519–20.
25. Hans M, Shimoni K, Danino D, Siegel SJ, Lowman A. Synthesis and characterization of mPEG-PLA prodrug micelles. Biomacromolecules. 2005;6(5):2708–17.
26. Shi W, Dolai S, Rizk S, Hussain A, Tariq H, Averick S, L'Amoreaux W, El Idrissi A, Banerjee P, Raja K. Synthesis of monofunctional curcumin derivatives, clicked curcumin dimer, and a PAMAM dendrimer curcumin conjugate for therapeutic applications. Org Lett. 2007;9(26):5461–4.
27. Li S, Vert M. Synthesis, characterization, and stereocomplex-induced gelation of block copolymers prepared by ring-opening polymerization of l(d)-lactide in the presence of poly(ethylene glycol). Macromolecules. 2003;36(21):8008–14.
28. Zhang X, Li Y, Chen X, Wang X, Xu X, Liang Q, Hu J, Jing X. Synthesis and characterization of the paclitaxel/MPEG-PLA block copolymer conjugate. Biomaterials. 2005;26(14):2121–8.
29. Zhu W, Li Y, Liu L, Zhang W, Chen Y, Xi F. Biamphiphilic triblock copolymer micelles as a multifunctional platform for anti-cancer drug delivery. J Biomed Mater Res A. 2011;96A(2):330–40.
30. Date AA, Nagarsenker MS, Patere S, Dhawan V, Gude RP, Hassan PA, Aswal V, Steiniger F, Thamm J, Fahr A. Lecithin-based novel cationic nanocarriers (Leciplex) II: improving therapeutic efficacy of quercetin on oral administration. Mol Pharm. 2011;8(3):716–26.
31. Prajapati RN, Tekade RK, Gupta U, Gajbhiye V, Jain NK. Dendimer-mediated solubilization, formulation development and *in vitro-in vivo* assessment of piroxicam. Mol Pharm. 2009;6(3):940–50.
32. Kwon GS, Okano T. Soluble Self-assembled block copolymers for drug delivery. Pharm Res. 1999;16(5):597–600.
33. Klibanov AL, Maruyama K, Torchilin VP, Huang L. Amphipathic polyethyleneglycols effectively prolong the circulation time of liposomes. FEBS Lett. 1990;268(1):235–7.
34. Torchilin V. Micellar nanocarriers: pharmaceutical perspectives. Pharm Res. 2007;24(1):1–16.
35. Zhang L, Eisenberg A. Multiple morphologies of "crew-cut" aggregates of polystyrene-b-poly(acrylic acid) block copolymers. Science. 1995;268(5218):1728–31.
36. Tobio M, Gref R, Sanchez A, Langer R, Alonso MJ. Stealth PLA-PEG nanoparticles as protein carriers for nasal administration. Pharm Res. 1998;15(2):270–5.
37. Parikh T, Bommana MM, Squillante III E. Efficacy of surface charge in targeting pegylated nanoparticles of sulpiride to the brain. Eur J Pharm Biopharm. 2010;74(3):442–50.
38. Dong Y, Feng SS. Methoxy poly(ethylene glycol)-poly(lactide) (MPEG-PLA) nanoparticles for controlled delivery of anticancer drugs. Biomaterials. 2004;25(14):2843–9.
39. Gref R, Miralles G, Dellacherie E. Polyoxyethylene-coated nanospheres: effect of coating on zeta potential and phagocytosis. Polym Int. 1999;48(4):251–6.
40. Lee J, Cho EC, Cho K. Incorporation and release behavior of hydrophobic drug in functionalized poly(d, l-lactide)-block-poly (ethylene oxide) micelles. J Control Release. 2004;94(2–3):323–35.
41. Allen C, Maysinger D, Eisenberg A. Nano-engineering block copolymer aggregates for drug delivery. Colloids Surf B. 1999;16(1–4):3–27.
42. Nagarajan R, Ganesh K. Block copolymer self-assembly in selective solvents: theory of solubilization in spherical micelles. Macromolecules. 1989;22(11):4312–25.
43. Kim SH, Tan JPK, Nederberg F, Fukushima K, Colson J, Yang C, Nelson A, Yang YY, Hedrick JL. Hydrogen bonding-enhanced micelle assemblies for drug delivery. Biomaterials. 2010;31 (31):8063–71.
44. Lee ALZ, Venkataraman S, Sirat SBM, Gao S, Hedrick JL, Yang YY. The use of cholesterol-containing biodegradable block copolymers to exploit hydrophobic interactions for the delivery of anti-cancer drugs. Biomaterials. 2012;33(6):1921–8.
45. Wang YJ, Pan MH, Cheng AL, Lin LI, Ho YS, Hsieh CY, Lin JK. Stability of curcumin in buffer solutions and characterization of its degradation products. J Pharm Biomed Anal. 1997;15(12):1867–76.
46. Yallapu MM, Ebeling MC, Chauhan N, Jaggi M, Chauhan SC. Interaction of curcumin nanoformulations with human plasma proteins and erythrocytes. Int J Nanomedicine. 2011;6:2779–90.
47. Shuai X, Ai H, Nasongkla N, Kim S, Gao J. Micellar carriers based on block copolymers of poly(epsilon-caprolactone) and poly (ethylene glycol) for doxorubicin delivery. J Control Release. 2004;98(3):415–26.
48. Luo L, Tam J, Maysinger D, Eisenberg A. Cellular internalization of poly(ethylene oxide)-b-poly(ε-caprolactone) diblock copolymer micelles. Bioconjugate Chem. 2002;13(6):1259–65.
49. Aryal S, Hu CMJ, Zhang L. Polymeric nanoparticles with precise ratiometric control over drug loading for combination therapy. Mol Pharm. 2011;8(4):1401–7.
50. Savic R, Luo L, Eisenberg A, Maysinger D. Micellar nanocontainers distribute to defined cytoplasmic organelles. Science. 2003;300 (5619):615–8.